

DESIGN OF A WIDEBAND BANDPASS FILTER WITH NOTCH-BAND USING SPURLINES

MEHDI SEPAHVAND ^{1*} and AKRAM SHEIKHI ²

^{1,2} Electrical Engineering Department, Faculty of Engineering, Lorestan University, Khorramabad, Iran.
Email: ¹sepahvand.mhd@fe.lu.ac.ir, ²sheikhi.a@lu.ac.ir

Abstract

In this paper, a simple structure bandpass filter with an ultra-wideband range from 4.73 GHz to 10 GHz and a notched band at 7.18 GHz has been introduced. Spurlines and coupled lines are used for the UWB response. The bandwidth and the notched band can be set at the desired frequency by the lengths and the width of spurlines. By adding L-shaped open stubs to the multi-mode resonator, the stopband rejection has been improved. Finally, one prototype is designed, manufactured, and measured, with results of 72.19% fractional bandwidth at the central frequency of 7.3 GHz, 0.5 dB insertion loss (IL), and return loss (RL) of -27 dB; this proves the feasibility and reliability of this filter.

Keywords: Bandpass filter; Notched band; Parallel-couple line; Ultra-wideband

1. INTRODUCTION

The design of bandpass filters (BPFs) is a well-known area with various uses in telecommunications, defense, and security. The essential parameters of the filter are bandwidth, compactness, low fabrication cost, etc. Different structures have been introduced to develop ultra-wideband (UWB) filters [1]–[12]. An ultra-wide stopband bandpass filter with a compact size has been designed in [1]. In [2], new configurations have been introduced to develop S-band BPF with a frequency range of 2–4 GHz. In [3], two compact-size wideband BPFs with common-mode suppression, and high selectivity are introduced. In [4], a simple method to design a dual-wideband bandpass filter is proposed. Due to interference between the undesired signals and the UWB range defined by U.S. Federal Communications Commission (FCC), a single- or multi-notched band filter is necessary to reject these signals. A compact UWB-BPF with an asymmetric coupled line structure and a notched band has been presented in [5]. However, the stopband rejection is not good. In [6], a compact UWB BPF using a hybrid microstrip and coplanar waveguide (CPW) with a narrow notched band has been proposed. A notched band BPF using a lowpass filter (LPF) coupled to the high-pass section is reported in [7]. In [8], a multi-notched band filter has been designed. In [9], a BPF with a notched band at 5.5 GHz is proposed by embedding a spurline within a multi-mode resonator (MMR). A tunable wideband BPF using the parallel-coupled line and cross-shaped resonator is presented in [10]. The dual-band BPF with good common-mode suppression and good differential-mode selectivity is achieved in [11]. In [12], new reconfigurable-bandwidth BPFs using parallel-coupled lines and cross-shaped resonators with control of the notched band are presented. All reported designs have an acceptable passband response with reasonably notched fractional bandwidth but without a good rejection level at the stopband region.

In this paper, a BPF with a notched band at 7.18 GHz consists of two asymmetrical couple lines as the input and output ports, and MMRs with two resonant modes have some spurlines has been proposed. The spurlines are created to eliminate the potential interference in the passband region. The proposed UWB bandpass filter is simulated and fabricated on a Rogers 4003C substrate with a height of 0.508 mm and the dielectric constant $\epsilon_r=3.55$.

2. ANALYSIS OF MMR

In this section, the details of the proposed resonator and filter design are illustrated. Firstly, the MMR to obtain the desired passband has been introduced and tries to allocate the resonant modes inside the desired passband. Then, the notched BPF design was presented. The first BPF in Fig 1, has the optimized parameters of $w_1=0.1$ mm, $l_1=4.2$ mm, $w_2=1.6$ mm, $l_2=7.5$ mm, and $d=0.2$ mm. The central structure resembles the stepped impedance resonator (SIR). Fig 2, shows the structure and equivalent circuit of the MMR.

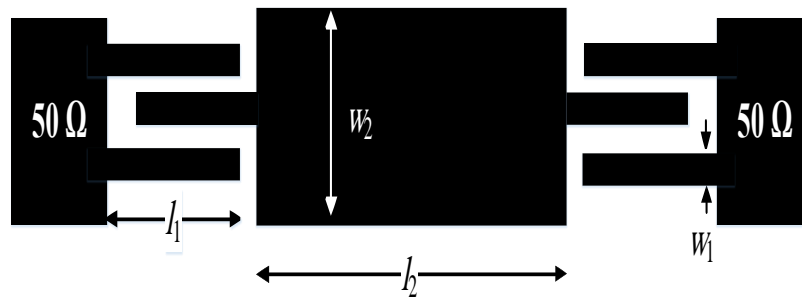


Figure 1: Structure of the first proposed filter

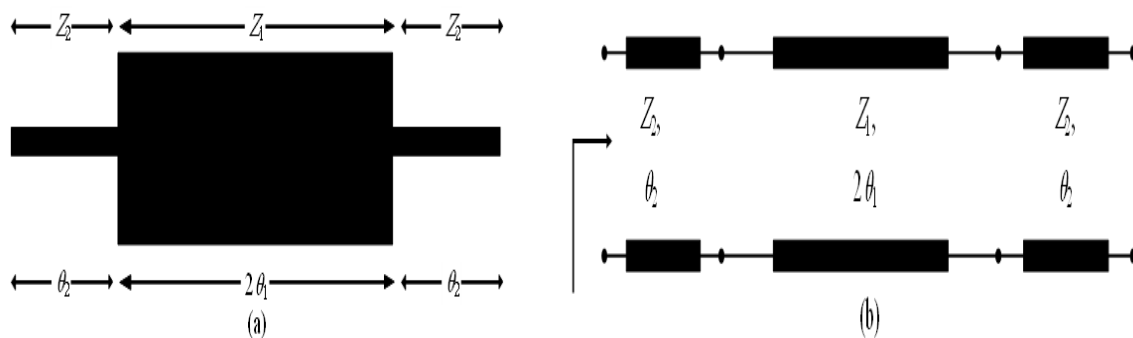


Figure 2: Structure of the first proposed filter

It consists of two sections with electrical characteristics of $(Z_1, 2\theta_1)$ and (Z_2, θ_2) . The main aim of the SIR is to obtain the larger frequency gap between the first and the second resonant modes. Generally, in the UWB filter, resonant modes of the resonator and frequency-dispersive characteristics of the coupled lines are generating an ultra-wide passband. The input admittance Y_{in} of the equivalent circuit in Fig 2(b) can be obtained as

$$Y_{in} = jY_2 \frac{2(R \tan \theta_1 + \tan \theta_2)(R - \tan \theta_1 \tan \theta_2)}{R(1 - \tan^2 \theta_1)(1 - \tan^2 \theta_2) - 2(1 + R^2) \tan \theta_1 \tan \theta_2} \quad (1)$$

Where $R=Z_2/Z_1$. At the resonances,

$$Y_{in} = 0 \quad (2)$$

From Eq. (1) and Eq. (2), a set of resonance frequencies (f_1 , f_2 , and f_3) can be evaluated. In the case when $\theta_2=2\theta_1=\theta$, we have

$$\theta(f_1) = \tan^{-1} \sqrt{\frac{R}{R+2}} \quad (3a)$$

$$\theta(f_2) = \tan^{-1} \sqrt{\frac{R+2}{R}} \quad (3b)$$

$$\theta(f_3) = \frac{\pi}{2} \quad (3b)$$

Ultra-wide passband results are obtained with good insertion loss S_{21} . The simulated reflection coefficient S_{11} and insertion loss S_{21} of the filter are shown in Fig 3. Three transmission poles at $f_1=5.6$ GHz, $f_2=10.3$ GHz, and $f_3=14.5$ GHz signify the three resonant modes (f_1 , f_2 , and f_3) of the stepped impedance MMR. The cut-off frequencies of the passband have been provided by the first and second-order resonant frequencies.

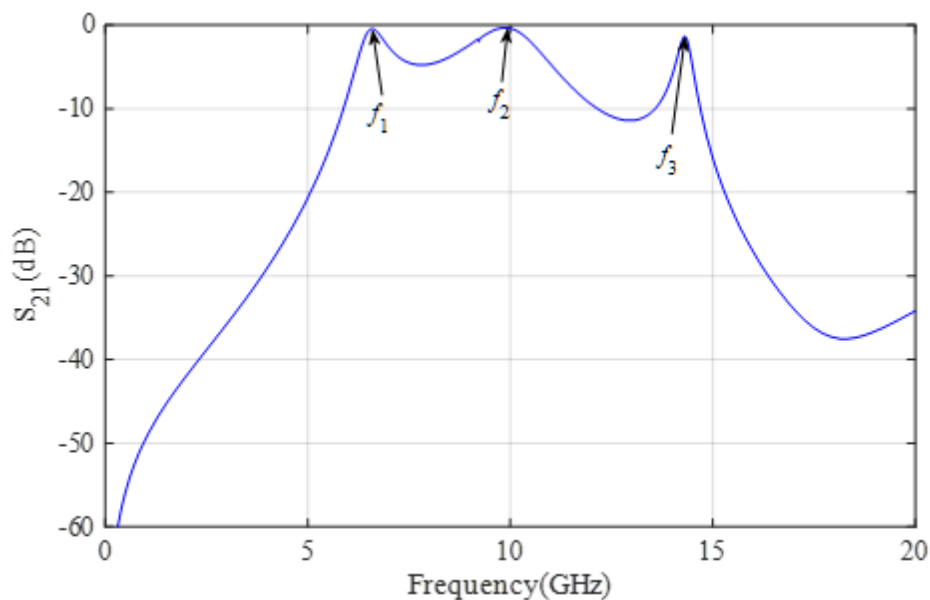


Figure 3: Simulated S_{21} of the first filter

3. UWB BPE design with notched band

The microstrip couple lines are made from single transmission line segments, which are equivalent to “ π ” lumped-element networks, Fig 4(a). In particular, a three-coupled line can be modeled by the circuit equivalent network, as shown in Fig 4(b). L_s and C_p are the self-capacitance and inductance of one of the lines, and M and C_c are the mutual inductance and capacitance between the coupled lines.

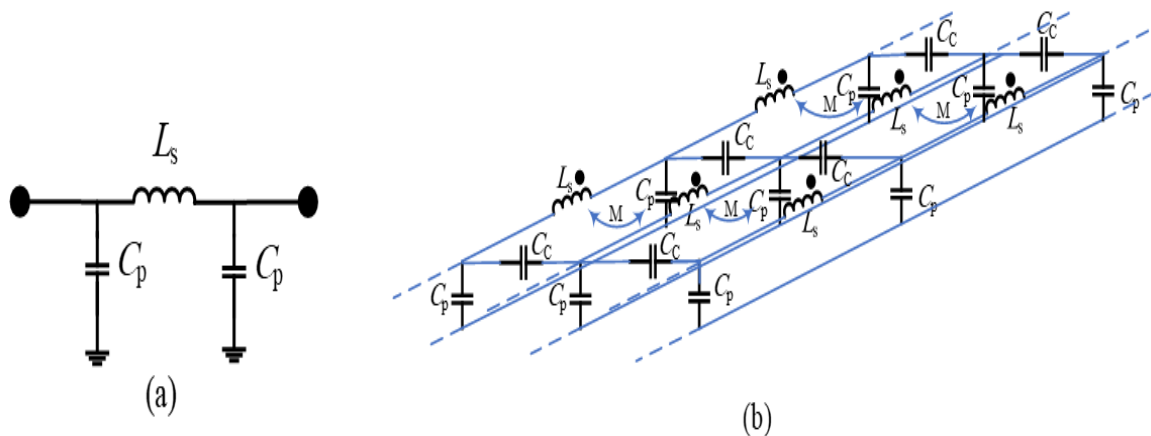


Fig 4: Equivalent circuit model of (a) single, and (b) three coupled lines



Fig 5: (a) Spurline resonator, (b) Equivalent circuit of spurlines

Fig 5 shows microstrip spurline sections and their equivalent circuits. The resonator circuits L_1C_1 and L_2C_2 represent the dual-band gap. characteristic, and the resistors R_1 and R_2 represent the radiation effect and transmission loss, which can be obtained as [13].

$$R_i = \left(\frac{1}{|S_{21,i}|} - 1 \right) 2Z_0 \Big|_{f=f_i} \quad (4)$$

$$C_i = \sqrt{\frac{-4Z_0^2}{2.83\pi Z_0 R_i \Delta f_i} + \frac{(R_i + 2Z_0)^2}{2}} \quad (5)$$

$$L_i = \frac{1}{4(\pi f_0)^2 C_i}, \quad i = 1, 2 \quad (6)$$

Where Δf_i is the bandwidth at the resonant frequency of f_i , and Z_0 is the characteristic impedance.

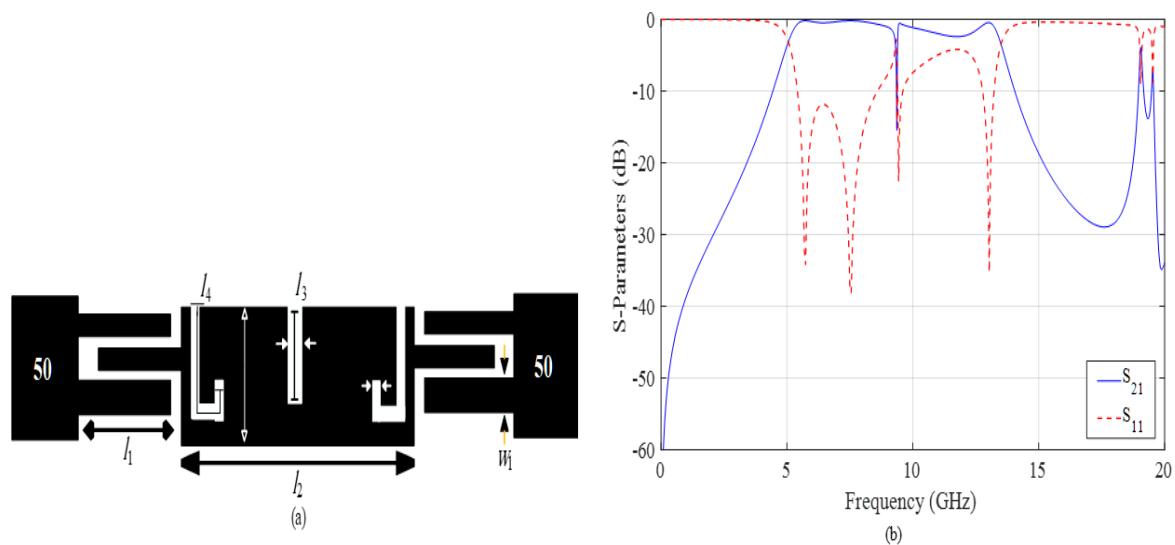


Fig 6: (a) Configuration of the proposed UWB filter (Filter 2), and (b) Simulated S_{21} and S_{11}

The structure of the proposed UWB filter as Filter 2 is shown in Fig 6(a). The optimized parameters of the filter are $w_1=0.2$ mm, $l_1=5$ mm, $w_2=1.4$ mm, $l_2=7.5$ mm, $w_3=0.2$ mm, $l_3=1$ mm, $l_4=1.5$ mm, $w_4=0.1$ mm, and $d=0.1$ mm. The simulated insertion loss S_{21} of the filter is shown in Fig. 6(b). According to Fig 6(b), the proposed structure has three drawbacks: a) high return loss in the bandpass. b) Low attenuation level in the stopband region. c) Low selectivity

at upper frequency. The open stubs with dimensions of $l_5=3.38$ mm, and $w_5=0.1$ mm have been added to the coupled line sections as Filter 3 (Fig 7(a)). The frequency response of Filter 3 is shown in Fig 7(b). Compared with Fig 6(b), it can be seen that the notched band with a better attenuation level has been generated.

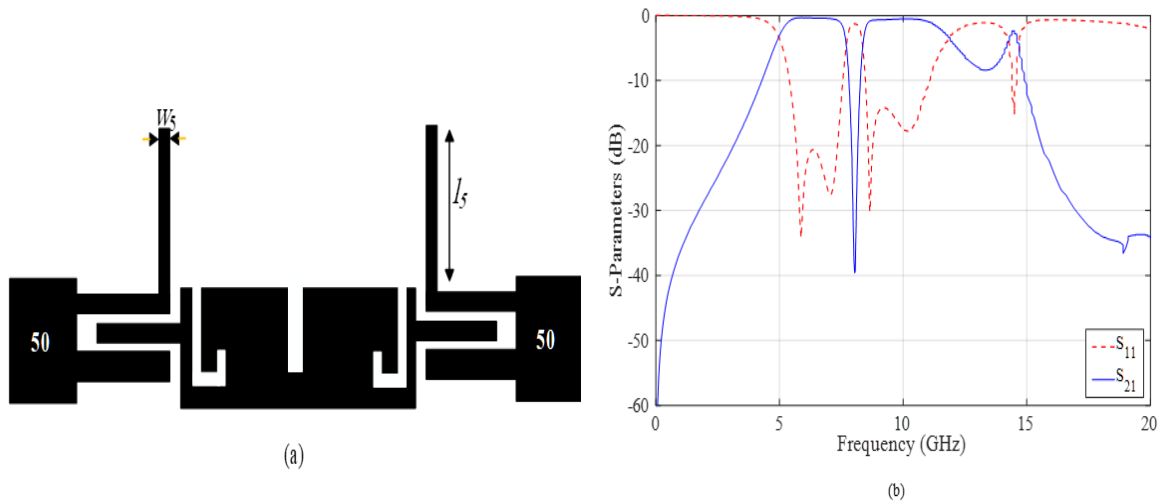


Fig 7: (a) Configuration of the UWB Filter 3, and (b) Simulated S_{21} and S_{11}

4. Simulation and Measurement Results

The stopband bandwidth of Filter 3 (as shown in Fig 7(b)) can be extended by open stubs because of the mutual suppression of spurious passband. Therefore, L-shaped open stubs are embedded in the input and output coupled lines with dimensions of $w_6=0.2$ mm, and $l_6=3.8$ mm. The configuration and photograph of the proposed filter are shown in Fig 8. Fig 9(a) shows the simulated insertion loss with varied l_6 . As can be seen, the attenuation level at the stopband region and fractional bandwidth can be improved by decreasing the length l_6 . The simulated S_{11} with different w_3 is recorded in Fig 9(b).

As illustrated, the return loss at the upper side passband is increased by a w_3 decrement and vice versa, while the return loss at the lower side passband doesn't change significantly. Simulated and measured S_{21} and S_{11} are shown in Fig 10(a). There is a deep downward notch at 7.18 GHz with -57 dB insertion loss. Fig 10(b) shows the group delay has a peak of 0.76 ns in the ultra-wideband range. The good performance of the proposed filter compared to other work is shown in Table 1.

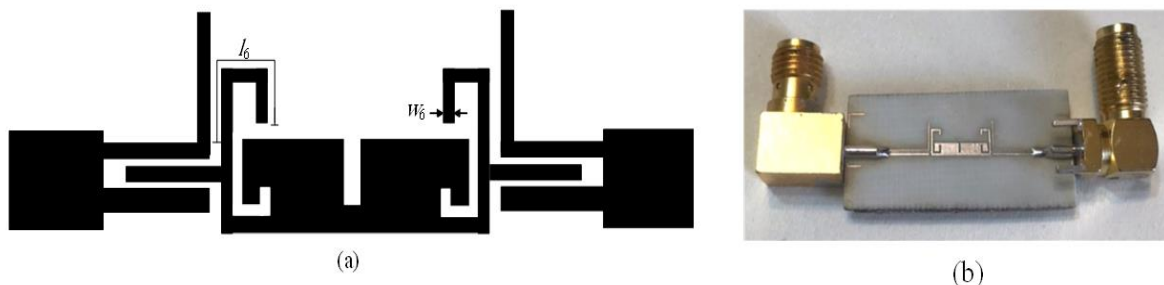


Fig 8: (a) Geometry, and (b) fabricated filter

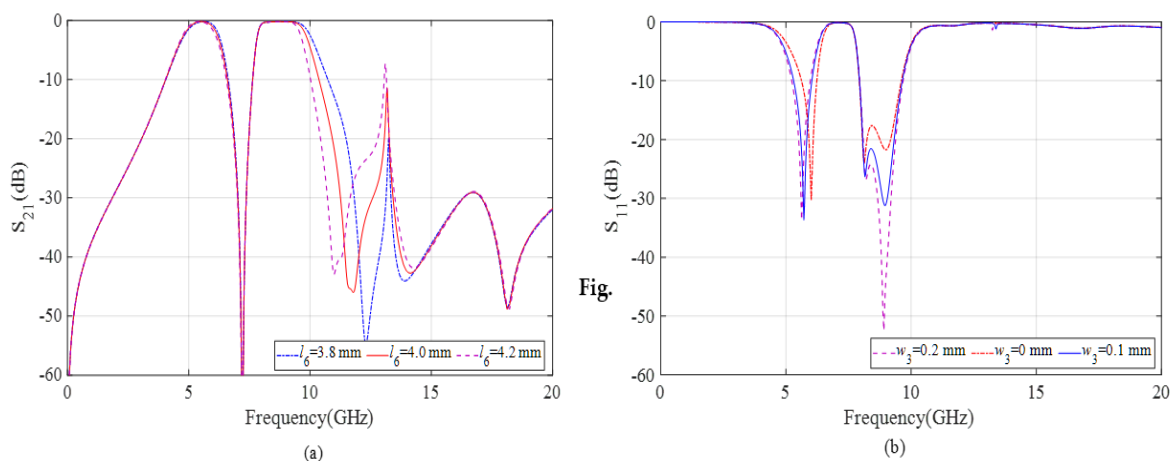


Fig 9: (a) S_{21} as a function of l_6 , and (b) S_{11} as a function of w_3

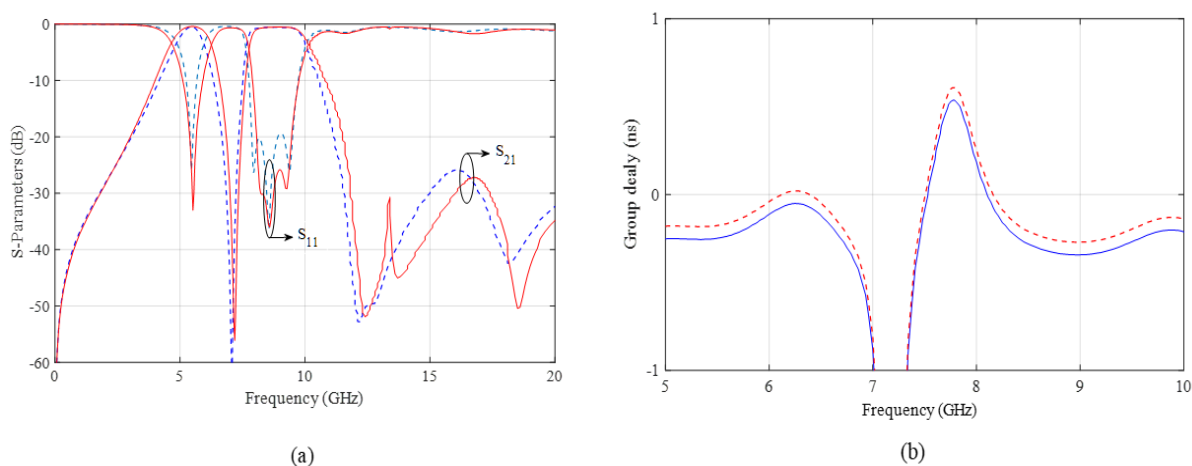


Fig 10: (a) Simulated and measured S_{21} and S_{11} , and (b) group delay

Table 1: Comparison with previous reported works

Ref.	CF (GHz)	Number of Tuning elements	Number of Notch bands	Notch Freq. (GHz)	GD (ns)	RL (dB)	IL (dB)	FBW (%)	Circuit size ($\lambda_g \times \lambda_g$)
[2]	3.0	No	No	No	0.6	11	1.0	66	0.23×0.073
[4]	2.4/5.2	No	No	No	4.6/ 5.5	22.1/20.8	0.3/0.7	51.9/23.3	0.28×0.20
[5]	6.6	No	1	6.3	0.3	10	0.5	121	0.94×0.10
[6]	6.84	No	1	5.80	0.28	14.3	0.9	113.5	0.303×0.166
[8]	6	No	3	3.6/5.3/8.4	< 0.4	> 11	< 1.25	80	0.74×0.61
[9]	5.5	No	1	5.5	0.4	12	0.9	107.6	0.27×0.10
[10]	6	3	1	5.0-8.2	< 2.8	10	< 2.6	41.7-96.7 (55)	0.32×0.15
Filter I in [12]	2.97	0	1	3.01	< 0.47	> 10	0.5	82.6	0.62×0.48
Filter II in [12]	2.94	2	1	3.02	< 3.9	> 15	1	41.6-83.4 (41.8)	0.62×0.48
Filter III in [12]	2.95	1	1	3.00	< 4.3	< 15	> 1	54.9-70.9 (15.6)	0.62×0.48
This Work	7.3	No	1	7.18	< 0.8	27	0.5	72.19	0.28×0.071

The meaning of abbreviations utilized in the table: Ref.—reference, CF. —center frequency, GD. — group delay, RL. — return loss, IL. — Insertion loss, FBW. —fractional bandwidth.

5. CONCLUSIONS

In this paper, a notched band filter based on the MMR has been presented. A deep notch at 7.18 GHz with -57 dB insertion loss has been created by spurlines. The design is economical because of using substrate Rogers 4003. The proposed UWB notch BPF has important features such as size compactness, low insertion loss, and high return loss. This filter is a good candidate for use in the UWB system to mitigate interference with narrowband systems such as *wireless local-area networks*.

References

- 1) A. Sheikhi, A. Alipour, and A. Mir, "Design and fabrication of an ultra-wide stopband compact bandpass filter," *IEEE Trans. Circuits Syst. II Exp. Briefs*, Vol. 67, No. 2, pp. 265–269, Mar. 2019. [CrossRef]
- 2) H. Shaman, "New S-Band Bandpass Filter (BPF) With Wideband Passband for Wireless Communication Systems," *IEEE Microw. Wireless Compon. Lett.*, vol. 22, no. 5, pp. 242–244, May. 2012. [CrossRef]
- 3) K. Aliqab and J. Hong, "Wideband Differential-Mode Bandpass Filters with Stopband and Common- Mode Suppression," *IEEE Microw. Wireless Compon. Lett.*, vol. 30, no. 3, pp. 233–236, Mar. 2020. [CrossRef]
- 4) G.-Z. Liang and F.-C. Chen, "A Compact Dual-Wideband Bandpass Filter Based on Open-/Short-Circuited Stubs," *IEEE Access*, vol. 8, pp. 20488–20492, Jan. 2020. [CrossRef]
- 5) H. Shaman and J.-S. Hong, "Asymmetric Parallel-Coupled Lines for Notch Implementation in UWB Filters," *IEEE Microw. Wireless Compon. Lett.*, Vol. 17, No. 7, pp. 516–518, Jul. 2007. [CrossRef]
- 6) X. Luo, J.-G. Ma, K. Ma, and K. S. Yeo, "Compact UWB Bandpass Filter with Ultra Narrow Notched Band," *IEEE Microw. Wireless Compon. Lett.*, vol. 20, no. 3, pp. 145–147, Mar. 2010. [CrossRef]
- 7) R. Ghatak, P. Sarkar, and D. R. Poddar, "A Compact UWB Bandpass Filter with Embedded SIR as Band Notch Structure," *IEEE Microw. Wireless Compon. Lett.*, vol. 21, no. 5, pp. 261–263, May. 2011. [CrossRef]
- 8) S. Kumar, R. Gupta, and M. S. Parihar, "Multiple Band Notched Filter Using C-Shaped and E-Shaped Resonator for UWB Applications," *IEEE Microw. Wireless Compon. Lett.*, vol. 26, no. 5, pp. 340–342, May. 2016. [CrossRef]
- 9) A. Neogi, J. R. Panda, S. Sil, S. Chakraborty, A. Tarafdar, "A UWB Band-pass Filter with a WLAN Notch based on Multi-Mode Resonator Structure for Application in Wireless Communication," in *Proc. IEEE International Conference on Applied Devices for Integrated Circuit (DevIC)*, Kalyani, India, 23rd-24th Mar 2019. [CrossRef]
- 10) CH. Teng, P. Cheong, S.-K. Ho, K.-W. Tam, and W.-WA. Choi, "Design of Wideband Bandpass Filter With Simultaneous Bandwidth and Notch Tuning Based on Dual Cross-Shaped Resonator," *IEEE Access*, vol. 8, pp. 27038–27046, Feb. 2020. [CrossRef]
- 11) X. Gua, B. Zhao, and B. Ren, "Dual-Band Differential Bandpass Filters Using Quadruple-Mode Stubs-Loaded Ring Resonator with Intrinsic Common-Mode Suppression for 5G," *IEEE Access*, vol. 8, pp. 205550–205557, Nov. 2020. [CrossRef]
- 12) X.-K. Bi, X. Zhang, S.-W. Wong, S.-H. Guo, and T. Yuan, "Design of Notched-Wideband Bandpass Filters with Reconfigurable Bandwidth Based on Terminated Cross-Shaped Resonators," *IEEE Access*, vol. 8, pp. 37416–37427, Mar. 2020. [CrossRef]
- 13) D.M. Pozar, *Microwave engineering*, 2nd ed., Wiley, NY, 1998.